Inorganic Chemistry

Article

pubs.acs.org/IC

Synthesis and Reactivity of New Bis(N-heterocyclic carbene) Iridium(I) Complexes

David J. Nelson, Byron J. Truscott, Alexandra M. Z. Slawin, and Steven P. Nolan*

EaStCHEM, School of Chemistry, University of St Andrews, North Haugh, St Andrews, Fife KY16 9ST, United Kingdom

Supporting Information

ABSTRACT: New complexes of the type *trans*-[IrCl(η^2-COE)(NHC)$_2$] (COE = *cis*-cyclooctene; NHC = N-heterocyclic carbene) have been prepared in one step from the reaction of ca. 4 equiv of NHC or [AgCl(NHC)] with [IrCl(η^2-COE)$_2$]$_2$ in benzene. These new complexes have been characterized by techniques including NMR and IR spectroscopy, X-ray crystallography, and elemental analysis. Exposing *trans*-[IrCl(COE)(I^{i}Pr^{Me})$_2$] to CO yielded *trans*-[IrCl(CO)(I^{i}Pr^{Me})$_2$], which is the only bis(NHC) analogue of Vaska's complex *trans*-[IrCl(CO)(PPh$_3$)$_2$] known to date. The synthesis of *trans*-[Ir(CO)(I^{i}Pr^{Me})$_2$(R)] (R = MeO, PhCC, OSiPh$_3$, O$_2$CPh) complexes has been achieved via deprotonation reactions involving the new hydroxide species *trans*-[Ir(OH)(CO)(I^{i}Pr^{Me})$_2$].

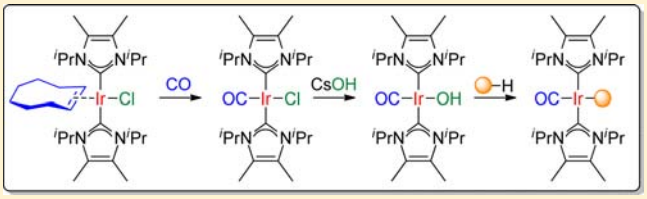

INTRODUCTION

The development of new catalytic methods is complemented by the discovery and exploration of new transition-metal complexes. The employment of *N*-heterocyclic carbenes (NHCs) as ligands represents one of the most important recent advances in transition-metal chemistry.[1] NHCs encompass a range of structural diversity and present opportunities for the fine tuning of ligand steric[2] and electronic[3] properties using the vast array of synthetic methodologies that is available.[4] Research within our group has focused on the exploration of the properties of NHCs, the metals to which they are coordinated, and the application of such complexes in homogeneous catalysis.

NHC−iridium(I) complexes of various types have been explored in the literature for a number of applications. For example, Kerr and co-workers have applied complexes of the type [Ir(η^4-COD)(NHC)(PR$_3$)][PF$_6$] (COD = 1,5-cyclooctadiene; PR$_3$ = PPh$_3$, PMe$_2$Ph, etc.) in H/D exchange[5] and hydrogenation[6] reactions, whereas Herrmann has utilized [Ir(η^4-COD)(NHC)$_2$][X] (X = BF$_4$, PF$_6$) complexes for C−H borylation reactions.[7,8] Earlier work from our group has shown the potential of [Ir(η^4-COD)(NHC)(py)][PF$_6$] complexes in hydrogenation,[9] transfer hydrogenation, and oxidation.[10] Recently, we reported the synthesis and characterization of [Ir(OH)(η^4-COD)(NHC)] complexes, which are highly versatile reagents for the activation of a variety of bonds.[11] In these species, the hydroxide moiety behaves as an internal base, capable of deprotonating a wide range of organic substrates, and this scaffold may have significant future applications in catalysis.

However, these examples all feature a COD ligand. In some reactions, this ligand may react with reagents such as hydrogen to yield *cis*-cyclooctene, which cannot reoccupy two coordination sites and, therefore, can potentially lead to catalyst decomposition. In addition, the two ligands in COD-bearing complexes are forced into a cis arrangement. A number of researchers have explored the use of structural motifs where COD is not present, such as complexes **1**−**3** (Chart 1). During

Chart 1. Cyclometalated Iridium(III) Complexes

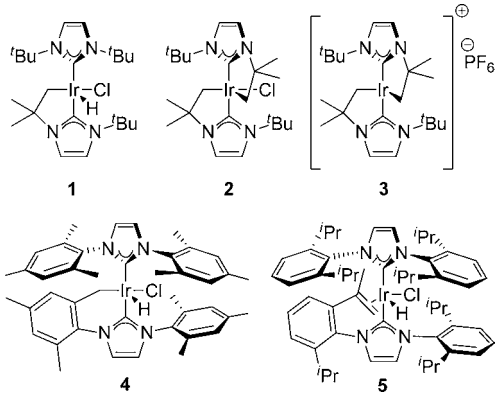

the synthesis of bis(NHC) complexes from [IrCl(η^2-COE)$_2$]$_2$ (COE = *cis*-cyclooctene), spontaneous insertion of the iridium center into the C−H bond of I^{t}Bu (1,3-bis(*tert*-butyl)imidazol-2-ylidene) was observed, generating the iridium(III)−hydride complex [IrClH(κ^2-I^{t}Bu)(I^{t}Bu)] (**1**).[12] A further period of stirring in solution resulted in the formation of the corresponding doubly cyclometalated complex [IrCl(κ^2-I^{t}Bu)$_2$] (**2**), whereas chloride abstraction with AgPF$_6$ led to the cationic 14-electron complex [IrCl(κ^2-ItBu)$_2$][PF$_6$] (**3**). Further studies of **1**−**3** established that the cyclometalation

Received: July 20, 2013
Published: October 22, 2013

   dx.doi.org/10.1021/ic4018773 | *Inorg. Chem.* 2013, 52, 12674−12681

event was reversible and that, under H_2, a dihydride complex stabilized by two agostic interactions could be isolated.[13] Under a D_2 atmosphere, the methyl groups of the NHC ligand were completely deuterated. This reversible reactivity with hydrogen has led to the use of this family of complexes in low loadings for H/D exchange[14,15] and the liberation of hydrogen from ammonia–borane.[16,17] Aldridge and co-workers have more recently prepared [IrClH(κ^2-IMes)(IMes)] (**4**; IMes = 1,3-bis(2,4,6-trimethylphenyl)imidazol-2-ylidene)[18] and [IrClH(κ^2-IPr)(IPr)] (**5**; IPr = 1,3-bis(2,6-diisopropylphenyl)imidazol-2-ylidene)[19] from the interaction of IMes and IPr, respectively, with $[IrCl(\eta^2\text{-COE})_2]_2$. However, although the interaction of bulky alkyl- and aryl-bearing NHCs with $[IrCl(\eta^2\text{-COE})_2]_2$ has been probed, the interactions of smaller alkyl-bearing NHCs have not been examined. We therefore sought to explore the synthesis and reactivity of new, COD-free bis(NHC)–iridium(I) complexes.

RESULTS AND DISCUSSION

***trans*-[IrCl(η^2-COE)(NHC)$_2$] Complexes.** Complexes bearing five different NHC ligands were prepared: I^{i}Pr (**6a**), I^{i}Pr^{Me} (**6b**), IsB (**6c**), ICy (**6d**), and IDD (**6e**) (I^{i}Pr = 1,3-bis(isopropyl)imidazol-2-ylidene; I^{i}Pr^{Me} = 1,3-diisopropyl-4,5-dimethylimidazol-2-ylidene; IsB = 1,3-diisobutylimidazol-2-ylidene; ICy = 1,3-dicyclohexylimidazol-2-ylidene; IDD = 1,3-dicyclododecylimidazol-2-ylidene) (Scheme 1). For complexes

Scheme 1. Preparation of Bis(NHC)–Ir Complexes

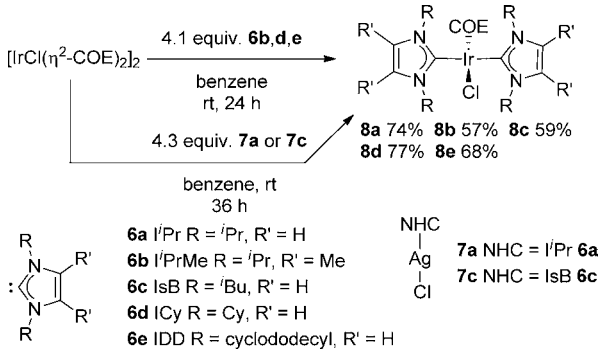

bearing I^{i}Pr^{Me}, ICy, and IDD, the free carbene and $[IrCl(\eta^2\text{-COE})_2]_2$ were stirred together in benzene for 24 h. The free carbenes I^{i}Pr and IsB are more difficult to prepare and purify, being oils that require distillation before use. Therefore, the corresponding [AgCl(NHC)] salts were employed as transmetalation reagents instead; these were prepared via the reaction of the corresponding NHC·HCl salt with silver(I) oxide.[20] No cyclometalation occurred during the syntheses of these complexes, and the corresponding *trans*-[IrCl(η^2-COE)(NHC)$_2$] complexes **8a–e** were obtained as analytically pure yellow solids after workup.

Full characterization was carried out using 1D and 2D ^{1}H and ^{13}C{^{1}H} NMR spectroscopic techniques, X-ray crystallography, and elemental analysis. The structures obtained through X-ray crystallographic analyses were consistent with the results of the elemental analyses (Figure 1; selected structural data can be found in Table 1, and experimental data can be found in Table 2). Although the small size of the crystals led to higher than desired values of R1 and wR2 and some difficulties in refinement (see the Experimental Section), sufficient data could be collected to discern the key structural features of the

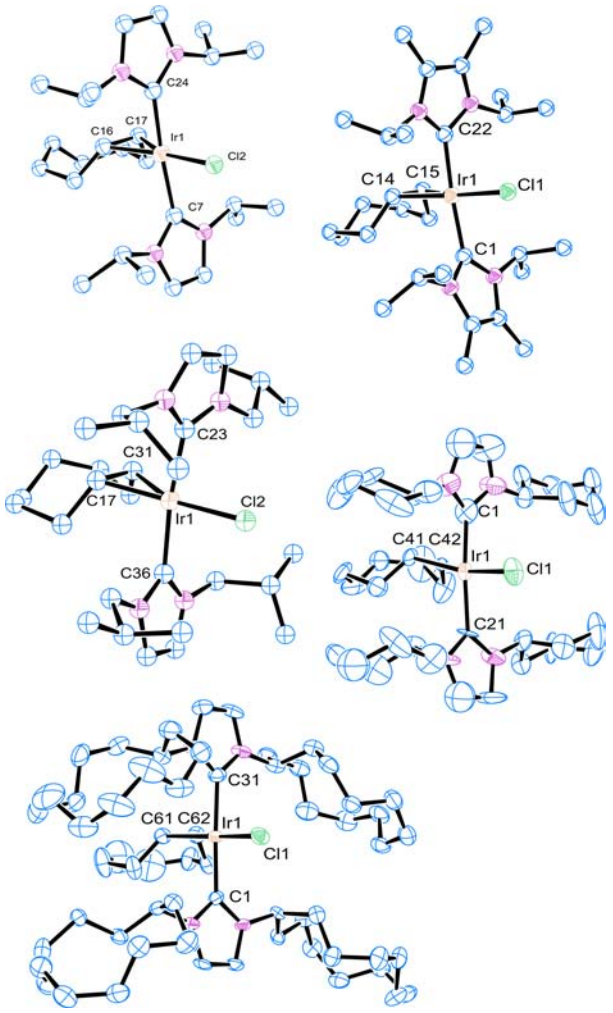

Figure 1. X-ray crystal structures of **8a–e**, showing 50% thermal ellipsoid probability. H atoms are excluded for clarity. More than one independent molecule is present in the unit cell for **8a–c**; therefore, only one example is presented here. See the CIF files (Supporting Information) for all independent molecules.

Table 1. Key Structural Parameters for 8a–e

complex	%V_{bur}[a]	C_{NHC1}–Ir–C_{NHC2} (deg)	Ir–C_{NHC1} (Å)	Ir–C_{NHC2} (Å)
8a	26.5; 26.1	173	2.05(2)	2.02(2)
		176	2.01(3)	2.09(3)
8b	28.2; 28.3	172	2.02(2)	2.01(2)
		172	2.07(2)	2.08(2)
		171	2.03(2)	2.03(2)
8c	27.1; 26.8	171	2.05(2)	2.04(2)
		175	2.06(2)	2.06(2)
8d	26.8; 26.8	173	1.98(2)	2.04(1)
8e	28.5; 29.4[b]	176	2.04(1)	2.04(1)

[a]Parameters: 3.5 Å sphere radius; 0.1 Å mesh spacing; H atoms excluded. [b]The two NHC ligands adopt considerably different conformations; see Figure 1.

complexes. As expected, the iridium(I) centers adopt a square-planar arrangement; the two NHC ligands are trans to each other, whereas the chloride ligand is located trans to the η^2-bound *cis*-cyclooctene ligand. The NHC ligands occupy the same plane, as opposed to **1–3**, where the NHC ligands occupy perpendicular planes.

dx.doi.org/10.1021/ic4018773 | Inorg. Chem. 2013, 52, 12674–12681

Table 2. Experimental Data for Single-Crystal X-ray Diffraction Analyses of 8a−e[a]

	8a	8b	8c	8d	8e
CCDC no.	948893	948894	948895	948896	948897
formula	$C_{26}H_{46}ClIrN_4$	$C_{30}H_{54}ClIrN_4$	$C_{30}H_{54}ClIrN_4$	$C_{40}H_{68}ClIrN_4$	$C_{62}H_{110}ClIrN_4$
formula wt	642.35	698.46	698.46	838.68	1139.25
color and habit	yellow prism	yellow prism	yellow needle	yellow prism	yellow prism
cryst dimens (mm)	0.030 × 0.030 × 0.030	0.120 × 0.120 × 0.030	0.100 × 0.010 × 0.010	0.200 × 0.200 × 0.200	0.100 × 0.030 × 0.030
crysta syst	monoclinic	monoclinic	orthorhombic	orthorhombic	triclinic
lattice type	*C*-centered	primitive	primitive	primitive	primitive
a (Å)	35.964(13)	28.701(5)	15.831(2)	10.527(2)	10.586(2)
b (Å)	9.425(3)	27.810(5)	23.242(3)	26.589(5)	14.087(3)
c (Å)	19.587(8)	13.601(3)	35.736(4)	15.428(2)	21.972(5)
α (deg)					100.058(7)
β (deg)	119.893(7)	94.994(4)			101.758(8)
γ (deg)					96.621(7)
V (Å^3)	5756(4)	10815(3)	13149(3)	4318.3(12)	3119(1)
space group	*Cc* (No. 9)	$P2_1/c$ (No. 14)	*Pbca* (No. 61)	$Pna2_1$ (No. 33)	$P\bar{1}$ (No. 2)
Z	8	12	16	4	2
D_{calcd} (g cm^{-3})	1.482	1.287	1.411	1.290	1.213
F_{000}	2592.00	4272.00	5696.00	1732.00	1208.00
μ(Mo Kα) (cm^{-1})	47.638	38.089	41.770	31.917	22.266
no. of observns (all rflns)	9018	19206	11866	25479	11009
no. of variables	577	983	649	443	613
rflns/params	15.63	19.54	18.28	57.51	17.96
R1 ($I > 2.00\sigma(I)$)	0.0774	0.0962	0.0862	0.0609	0.0616
R1 (all reflections)	0.1043	0.1332	0.1538	0.0789	0.0820
wR2 (all reflections)	0.1906	0.2364	0.2087	0.1682	0.1729
goodness of fit indicator	1.088	1.130	1.108	1.110	1.107
max shift/error in final cycle	0.000	0.003	0.001	0.000	0.000
max peak in final diff map (e/Å^3)	2.07	1.72	1.92	2.02	2.04
min peak in final diff map (e/Å^3)	−1.72	−2.98	−1.99	−3.72	−1.36

[a]Further details can be found in the Experimental Section.

The high degree of flexibility associated with the *N* substituents in **8a−e** means that they may adopt conformations far away from the metal center. The *tert*-butyl groups in **1−3** rotate in very close proximity to the metal center, resulting in spontaneous C−H insertion processes. This type of behavior is similar to that observed in the case of the addition of free NHC ligands to $[Ni(CO)_4]$, where IAd (1,3-bis(adamantyl)imidazol-2-ylidene) and I^{t}Bu yielded complexes of the form $[Ni(CO)_2(NHC)]$ rather than the expected $[Ni(CO)_3(NHC)]$ species, due to the increased steric bulk very close to the metal center.[21] Despite the overall size of IDD, no cyclometalation occurs, most likely due to the considerable flexibility of this ligand.[22] It can be seen from the X-ray crystal structure that one ligand in **8e** adopts a conformation in which the cycloalkyl rings are far removed from the metal center, whereas the second ligand adopts an arrangement where the rings envelop the metal center. The buried volume percent values ($\%V_{bur}$)[2,23] of the two IDD ligands are therefore rather different (Table 1); one has a $\%V_{bur}$ value of 29.4%, the bulkiest example seen here, whereas the other has a $\%V_{bur}$ value of 28.5%, comparable to that of the smaller ligands. This fluctuating steric behavior is consistent with that observed in several organometallic complexes.[22] The ligands of the ICy complex (**8d**) exhibit slightly lower values for $\%V_{bur}$ than those in I^{i}Pr^{Me}-bearing **8b**, despite the larger *N* substituent in the former. Similar results have been reported by us for square-planar $[Ir(OH)(COD)(NHC)]$ complexes due to the steric repulsion exerted by methyl groups on the backbone of the NHC.[11,24] The Ir1−C1 bond length in **8d** is considerably shorter than the Ir1−C21 distance and shorter than the corresponding bond lengths in the other complexes. Although no clear explanation for this is apparent, it should be noted that such differences in bond lengths were recorded for complexes **2** and **3** and that DFT calculations suggested that NHC to metal π bonding was the root cause.[12] However, it should be noted that given the R1 and wR2 values obtained for these crystal structure determinations, particularly detailed comparisons of bond lengths and buried volumes are not possible. Instead, the data confirm the proposed structure and indicate that ligand steric bulk decreases here in the order IDD > I^{i}Pr^{Me} > ICy ≈ IsB ≈ I^{i}Pr.

Although $\%V_{bur}$ is a convenient metric for assessing the steric properties of ligands,[2] the construction of steric maps using the freely available SambVca software[23] allows the steric environment around the metal center to be visualized in three-dimensional space (Figure 2 shows the maps for the IDD ligands in **8e**). The construction of steric maps for each complex (see Figures S30−S33 in the Supporting Information for steric maps for **8a−d**) revealed that the NHCs in each complex have similar steric impacts on the metal center, within the 3.5 Å sphere considered. Steric bulk is usually focused in two opposite quadrants, suggesting that, if the *cis*-cyclooctene ligand were removed, the metal center should be more accessible than those of complexes **1−3**, due to the perpendicular arrangement of the latter.

With these new complexes structurally characterized, their reactivity was probed by exposing them to various reagents and conditions. The isolation of $[IrCl(\eta^2\text{-COE})(NHC)_2]$ complexes was consistent with the results reported by Aldridge et al.

dx.doi.org/10.1021/ic4018773 | Inorg. Chem. 2013, 52, 12674−12681

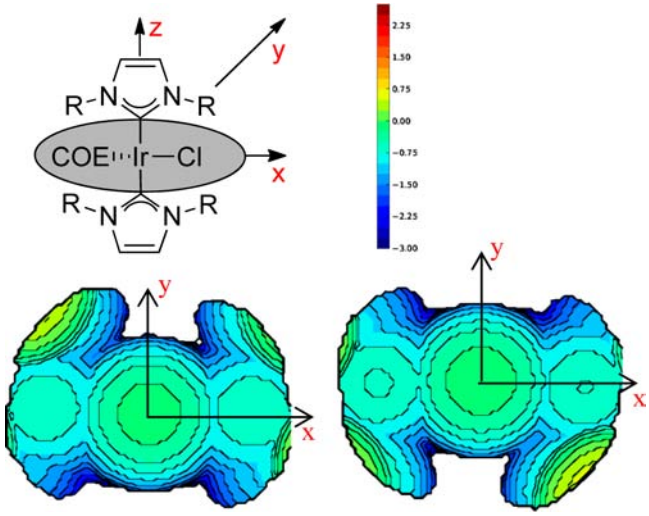

Figure 2. Steric maps of the IDD ligands in **8e**, calculated using the SambVca web application[23] (sphere radius 3.5 Å, mesh spacing 0.1 Å, hydrogen atoms omitted).

during the preparation of [IrClH(κ^2-IMes)(IMes)] (**4**), where the intermediate [IrCl(η^2-COE)(IMes)$_2$] (**8f**) was isolated and characterized; this was to date the only complex of this motif reported in the literature, and its reactivity and potential in catalysis was not explored. Aldridge et al. advanced **8f** to **4** by heating in THF solution (complete conversion after 24 h at 65 °C in toluene). Although small traces of hydride species were apparent after prolonged heating of **8a**,**e** (12 h at 90 °C), further heating (72 h at 90 °C) of **8a** led to decomposition, whereas **8e** gave ca. 50% conversion to iridium hydride species (δ_H(toluene-d_8) −32.3 and −32.4 ppm). The cyclometalation process is therefore far less facile for **8a**−**e** than for **8f**; the reactivity of **8a**−**e** is therefore likely to be quite different from that of complexes **1**−**5**.

Unfortunately, further attempts to probe the reactivity of these species were not particularly successful. Attempts to remove the chloride, either by substitution using CsOH in THF[11] or by chloride abstraction with NaB(Ar$_F$)$_4$ (Ar$_F$ = 3,5-bis(trifluoromethyl)phenyl) were not successful and resulted in recovered starting material or decomposition. Complexes **8a**−**e** are highly oxygen sensitive, even in the solid state, and rapidly turn green and then black on exposure to the ambient atmosphere. When a solution of **8b** was exposed to oxygen in an NMR tube with a J. Young valve, characteristic signals corresponding to free *cis*-cyclooctene were apparent, along with decomposition of the complex. The η^2-bound COE ligand therefore renders **8a**−**e** rather fragile. Exposure to hydrogen yielded a mixture of iridium hydride species, suggesting potential future applications of these species in H/D exchange and hydrogenation reactions. A trial reaction was conducted in which triphenylsilane successfully underwent H/D exchange catalyzed by [IrCl(η^2-COE)(ICy)$_2$] (**8d**) in 98% conversion (Scheme 3). This reactivity is at the very least equivalent to that

Scheme 3. H/D Exchange on Silanes Catalyzed by 8d

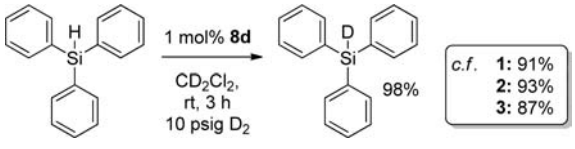

of complexes **1**−**3** under the same reaction conditions. These promising results in catalysis are currently under further investigation. However, further functionalization of the bis(NHC) species was desired, to explore their potential in organometallic chemistry.

***trans*-[IrCl(CO)(I^{i}Pr^{Me})$_2$]: A Bis(NHC) Analogue of Vaska's Complex.** When a benzene-d_6 solution of **8b** was exposed to CO at room temperature in an NMR tube fitted with a J. Young valve, we observed complete dissociation of the *cis*-cyclooctene ligand and slight upfield shifting of the NHC ligand resonances. After a preparative-scale reaction (in pentane solution) (Scheme 4), full characterization of the resulting pale

Scheme 4. Reaction between 8b and CO

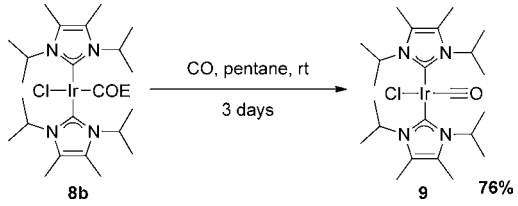

yellow solid by NMR spectroscopy, elemental analysis, and IR spectroscopy confirmed the identity of the species to be *trans*-[IrCl(CO)(I^{i}Pr^{Me})$_2$] (**9**).

IR analysis of this novel complex revealed the stretching frequency of the carbonyl ligand (ν_{CO}(CH$_2$Cl$_2$) 1917 cm^{-1}; ν_{CO}(*n*-hexane) 1929 cm^{-1}, at room temperature). This complex is the only bis(NHC) structural analogue of Vaska's complex[25] *trans*-[IrCl(CO)(PPh$_3$)$_2$] (**10**; ν_{CO}(CHCl$_3$) = 1967 cm^{-1}) reported to date. Liu and co-workers have reported [IrCl(CO)(NHC)(PR$_3$)] (PR$_3$ = PPh$_3$, PCy$_3$; NHC = 1,3-dibenzylimidazol-2-ylidene, 1,3-dibenzyl-4,5-dihydroimidazol-2-ylidene, 1,3-diethyl-4,5-dihydroimidazol-2-ylidene, 1,3-bis(methoxyethylene)-4,5-dihydroimidazol-2-ylidene, 1,3-bis(*o*-methoxybenzyl)-4,5-dihydroimidazol-2-ylidene) complexes.[26,27] IR measurements showed these mixed-ligand species to be approximately as electron rich as the corresponding bis(phosphine) species (Figure 3). **10** is a key model complex in organometallic chemistry, which has been used to study many fundamental processes.[25] Notably, the iridium center is more electron rich in **9** than in **10**, as determined from the lower ν_{CO} of the latter, due to back-bonding from the iridium d orbitals into the σ_{CO}* antibonding orbital. The value obtained is similar to that measured for [IrCl(CO)(PCy$_3$)$_2$] (**11**; ν_{CO}(CH$_2$Cl$_2$) 1922 cm^{-1}).[28] Therefore, although **9** is structurally related to Vaska's complex, its reactivity is likely to be quite different, due to the considerable steric differences between I^{i}Pr^{Me} and PPh$_3$, as well as the measured difference in the electronic nature of the iridium center.

Complex **9** was then exposed to some model reagents to understand its reactivity. Reaction with ca. 1 atm of H$_2$ at room temperature, 40 °C, or −78 °C did not yield any iridium hydride species despite the presence of a sharp ($\phi_{1/2}$ < 1 Hz at room temperature) ^{1}H resonance on the NMR spectrum corresponding to hydrogen (Scheme 5). This suggests that the equilibrium constant for oxidative addition of hydrogen (K_{eq}) is very low indeed. In the case of **10**, K_{eq} is ca. 10^5.[25] Vaska's complex is also known to react reversibly with O$_2$ to yield the dioxygen adduct. When **9** was exposed to oxygen, ^{1}H NMR signals corresponding to a new species appeared upfield of the signals for **9**, albeit very slowly (ca. 7−10 days under 1 atm of

dx.doi.org/10.1021/ic4018773 | Inorg. Chem. 2013, 52, 12674−12681

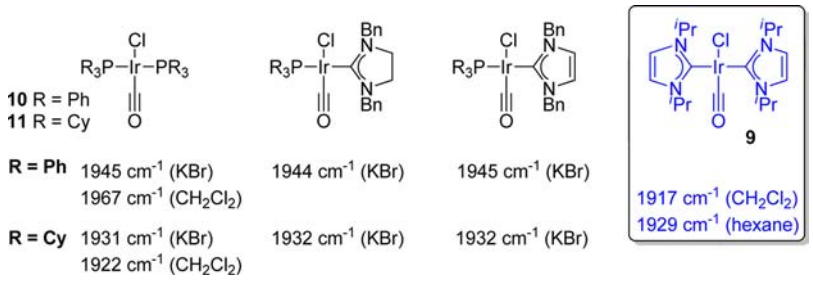

Figure 3. Comparison of IR spectroscopic data for a range of $[IrCl(CO)(L)_2]$ complexes (L = PR_3, NHC); the medium used is indicated in brackets.[26−28]

Scheme 5. Reactivity of 9 and 10 toward H_2 and O_2

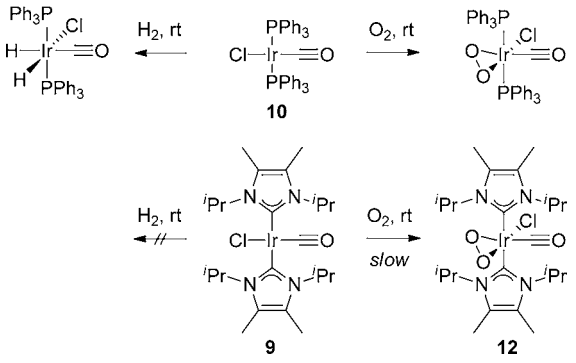

O_2 in CD_2Cl_2). This new complex may be the dioxygen complex $[IrCl(CO)(O_2)(I^iPr^{Me})_2]$ (**12**); however, although key ^1H NMR spectroscopic features could be identified, decomposition to a black precipitate on a similar time scale precluded isolation and further characterization. These data are sufficient to show that **9** is very much less reactive than Vaska's complex **10**.

This sluggish reactivity of **9** can be rationalized by comparing the structure with that of Vaska's complex **10** and PCy_3-bearing analogue **11**. NHC ligands are known to be capable of accepting π-electron density[29] and are therefore perhaps too soft to stabilize the iridium(III) products. This is despite the higher electron density at the metal center of **9**, as evidenced by the much lower value of ν_{CO}. However, Vaska and Chen reported that $[IrCl(CO)(P(o\text{-}MeC_6H_4)_3)_2]$ was almost completely unreactive with O_2, despite having electronic properties similar to those of **10**, suggesting that steric properties play a key role in these types of complexes.[30] **11** is also known to be poorly reactive with O_2, despite the increased electron richness of the iridium center in this species.[30] The steric bulk of **9**−**11** was assessed using buried volumes ($\%V_{bur}$) calculated with SambVca, using a DFT-derived structure of **9** (M06L/SDD, using Gaussian;[31] see the Supporting Information for details) and published structures of **10** and **11**.[32,33] The buried volumes were found to be 27.3%, 28.6%, and 29.0%, respectively (average of the two ligands in each complex), pointing to only marginal differences in steric impact. However, these measurements are based on solid state (or in the case of DFT calculations, gas phase) data and do not necessarily reflect solution state behavior.

Applying $[Ir(OH)(CO)(I^iPr^{Me})_2]$ in the Synthesis of New Organoiridium(I) Complexes. We have previously shown that iridium(I) hydroxide complexes are powerful intermediates for the preparation of a range of organoiridium(I) complexes, bearing various substituents including siloxides, aryl groups, amides, alkoxides, and alkynes.[11] We therefore sought to prepare a bis(NHC)−iridium(I) complex to evaluate the potential of this framework in bond activation reactions. The reaction between **8b** and CsOH often resulted in decomposition with the formation of free *cis*-cyclooctene. Hoping that replacement of the labile alkene with a carbonyl ligand might concentrate reactivity at the chloride, we exposed **9** to CsOH in THF in a manner analogous to that used previously.[11] In addition, the carbonyl ligand also provides a convenient spectroscopic handle. Gratifyingly, the desired hydroxide **13** could be obtained (Scheme 6a). A bond activation study was

Scheme 6. Preparation of Ir Hydroxide 13 from 9 and Reactivity of 13 toward Organic Substrates

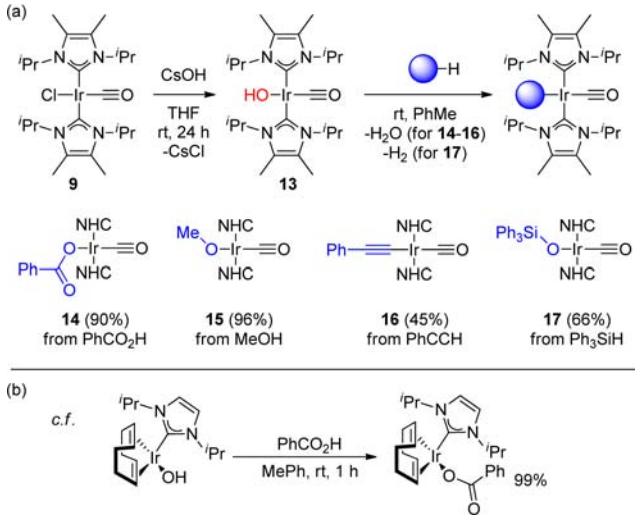

then undertaken with some representative substrates. Although deprotonation reactions with $[Ir(OH)(COD)(NHC)]$ were found to be clean and rapid (e.g., Scheme 6b),[11] often occurring within mixing time, the reactions with **13** were far more sluggish. Reactions were typically conducted neat, over ca. 24 h at room temperature.

The resulting organoiridium(I) complexes **14**−**17** were fully characterized using ^1H and $^{13}C\{^1H\}$ NMR spectroscopy and elemental analysis. Although the new hydroxide species **13** is less reactive than the corresponding $[Ir(OH)(COD)(NHC)]$ species, the isolation of the former complex suggests that the synthesis of a range of iridium(I) hydroxides should be possible from the corresponding chloride species. Complex **13** therefore allows access to a new range of organoiridium(I) species, bearing two NHC ligands.

dx.doi.org/10.1021/ic4018773 | Inorg. Chem. 2013, 52, 12674−12681

CONCLUSIONS

A series of complexes has been prepared and characterized, showing how the interaction between small NHC ligands and $[IrCl(\eta^2\text{-COE})_2]_2$ reproducibly yields *trans*-$[IrCl(\eta^2\text{-COE})(NHC)_2]$ complexes. Unlike the previously reported complexes **1**−**5**, where larger ligands such as IMes, I^{t}Bu, and IPr are employed, cyclometalation is far from facile.

The *trans*-$[IrCl(\eta^2\text{-COE})(NHC)_2]$ complexes thus formed were somewhat resistant to further functionalization, which is proposed to be due to facile dissociation of the η^2-COE ligand. Exposure of *trans*-$[IrCl(\eta^2\text{-COE})(I^iPr^{Me})_2]$ to CO yielded *trans*-$[IrCl(CO)(I^iPr^{Me})_2]$, which is the only bis(NHC) analogue of Vaska's complex reported to date. Although the reactivity of this complex was very limited, attributed to the soft NHC ligands being less able than phosphanes to stabilize iridium(III) products, it was robust enough to be straightforwardly converted to the corresponding hydroxide complex. This hydroxide species allowed access to a number of bis(NHC) organoiridium(I) complexes via established deprotonation routes, suggesting that it may be a useful reagent for the preparation of a range of new Ir(I) complexes.

Further investigations into the reactivity and applications of these novel complexes are currently underway in our laboratories.

EXPERIMENTAL SECTION

General Considerations. All manipulations were carried out in an Ar-filled glovebox using dry, degassed solvents unless otherwise stated. NMR spectra were recorded on Bruker 300, 400, or 500 MHz (^{1}H observe frequency) NMR spectrometers and referenced to residual solvent resonances.[34] All chemical shifts are given in ppm, and coupling constants are given in Hz. $[IrCl(\eta^2\text{-COE})_2]_2$ was prepared according to the literature method[35] and stored at −40 °C in the glovebox. [AgCl(NHC)] complexes were prepared according to the literature method.[20] IR spectroscopy was carried out using a Perkin-Elmer Paragon series 1000 FTIR spectrometer.

$[IrCl(\eta^2\text{-COE})(I^iPr)_2]$ (8a). Benzene (5 mL) was added to solid $[IrCl(\eta^2\text{-COE})_2]_2$ (99.3 mg, 0.111 mmol) and [AgCl(I^{i}Pr)] (141.9 mg, 0.480 mmol, 4.3 equiv) and stirred for 36 h at room temperature. Upon completion, the solution was filtered through Celite, and the solvent was removed in vacuo. The solid was washed carefully with cold (−40 °C) pentane (3 × 1 mL) and dried in vacuo. Yield: 104.5 mg (0.163 mmol, 74%) of a bright yellow powder. ^{1}H NMR (CD_2Cl_2, δ): 6.86 (s, 4H, N(C*H*)$_2$N), 6.06 (sept, $^3J_{HH}$ = 6.8, 4H, NC*H*(CH$_3$)$_2$), 2.17−2.08 (m, 2H, COE), 1.98−1.89 (m, 2H, COE), 1.50 (d, $^3J_{HH}$ = 6.8, 12H, NCH(C*H*$_3$)$_2$), 1.47−1.43 (m, 2H, COE), 1.37−1.22 (m, 4H, COE), 1.18−1.07 (m, 2H, COE), 0.93−0.77 (m, 2H, COE). ^{13}C{^{1}H} NMR (CD_2Cl_2, δ): 182.4 (Ir−C), 115.4 (N(CH)$_2$N), 51.4 (CH-(CH$_3$)$_2$), 35.9 (COE), 32.3 (COE), 31.0 (COE), 27.0 (COE), 24.3 (CH(CH$_3$)$_2$), 23.0 (CH(*C*H$_3$)$_2$). Anal. Calcd for $C_{26}H_{46}N_4ClIr$: C, 48.62; H, 7.22; N, 8.72. Found: C, 48.65; H, 6.87; N, 8.75. Crystals suitable for X-ray diffraction studies were grown by chilling a pentane solution to −40 °C.

$[IrCl(\eta^2\text{-COE})(I^iPr^{Me})_2]$ (8b). Benzene (2 mL) was added to solid $[IrCl(\eta^2\text{-COE})_2]_2$ (68.7 mg, 0.077 mmol) and I^{i}Pr^{Me} (58.1 mg, 0.322 mmol, 4.19 equiv) and stirred for 20 h at room temperature. The solvent was removed in vacuo, and the resulting solid was carefully washed with cold (−40 °C) pentane (3 × 1 mL) and dried in vacuo. Yield: 61.0 mg (0.087 mmol, 57%) of a bright yellow powder. ^{1}H NMR (CD_2Cl_2, δ): 6.60 (sept, $^3J_{HH}$ = 7.0, 4H, NC*H*(CH$_3$)), 2.17 (s, 12H, N(C(C*H*$_3$))$_2$N), 2.15−2.07 (m, 2H, COE), 1.96 (app d, J = 9.0, 2H, COE), 1.64−1.25 (m, 6H, COE), 1.59 (d, $^3J_{HH}$ = 7.0, 12H, CH(C*H*$_3$)$_2$), 1.45 (d, $^3J_{HH}$ = 7.0, 12H, CH(C*H*$_3$)$_2$), 1.22−1.08 (m, 2H, COE), 1.02−0.84 (m, 2H, COE). ^{1}H NMR (C_6D_6, δ): 6.96 (sept, $^3J_{HH}$ = 7.0, 4H, NC*H*(CH$_3$)), 2.49 (app d, 2H, J = 12.9, COE), 2.38 (app d, J = 10.0, 2H, COE), 1.81 (s, 12H, N(C(C*H*$_3$))$_2$N), 1.77−1.06 (m, 10H, COE), 1.66 (d, $^3J_{HH}$ = 6.9, 12H, CH(C*H*$_3$)$_2$), 1.51 (d, $^3J_{HH}$ = 7.2, 12H, CH(C*H*$_3$)$_2$). ^{13}C{^{1}H} NMR (CD_2Cl_2, δ): 182.0 (Ir−C), 123.1 (N(CCH$_3$)$_2$N), 52.1 (CH(CH$_3$)$_2$), 35.1 (COE), 32.2 (COE), 30.5 (COE), 26.7 (COE), 22.2 (CH(*C*H$_3$)$_2$), 21.5(CH(*C*H$_3$)$_2$), 10.2 (N(*C*CH$_3$)$_2$N). Anal. Calcd for $C_{30}H_{54}N_4ClIr$: C, 51.59; H, 7.79; N, 8.02. Found: C, 51.61; H, 7.64; N, 7.97. Crystals suitable for X-ray diffraction studies were grown by chilling a pentane solution to −40 °C.

$[IrCl(\eta^2\text{-COE})(IsB)_2]$ (8c). Benzene (5 mL) was added to solid $[IrCl(\eta^2\text{-COE})_2]_2$ (100.0 mg, 0.111 mmol) and [AgCl(IsB)] (154.7 mg, 0.478 mmol, 4.3 equiv) and stirred for 48 h at room temperature, with protection from light. Upon completion, the solution was filtered through Celite, and the solvent was removed in vacuo to yield an orange-yellow solid. This solid was extracted into pentane (3 × 5 mL), and the solution was filtered through Celite before being concentrated in vacuo. The residue was carefully washed with cold (−40 °C) pentane (2 × 1 mL) and dried in vacuo. Yield: 58.4 mg (0.084 mmol, 38%) of a bright yellow powder. ^{1}H NMR (CD_2Cl_2, δ): 6.80 (s, 4H, N(C*H*)$_2$N), 5.02−4.85 (m, 4H, NC*H*$_2$^{i}Pr), 4.01−3.86 (m, 4H, NC*H*$_2$^{i}Pr), 2.40 (sept, $^3J_{HH}$ = 6.8, 4H, C*H*(CH$_3$)$_2$), 2.15−2.03 (m, 2H, COE), 1.81−1.70 (m, 2H, COE), 1.46−1.17 (m, 6H, COE), 0.99 (dd, $^3J_{HH}$ = 6.8, 0.8, 24H, CH(C*H*$_3$)$_2$), 1.15−0.56 (m, 4H, COE). ^{13}C{^{1}H} NMR (CD_2Cl_2, δ): 184.6 (Ir−C), 119.0 (N(CH)$_2$N), 58.3(CH$_2$CH(CH$_3$)$_2$), 35.7 (COE), 30.8 (CH$_2$CH(CH$_3$)$_2$), 29.5 (COE), 27.0 (COE), 20.8 (CH$_2$CH(*C*H$_3$)$_2$), 20.7(CH$_2$CH(*C*H$_3$)$_2$). Crystals suitable for X-ray diffraction studies were grown by chilling a pentane solution to −40 °C.

$[IrCl(\eta^2\text{-COE})(ICy)_2]$ (8d). Benzene (2 mL) was added to solid $[IrCl(\eta^2\text{-COE})_2]_2$ (50.1 mg, 0.056 mmol) and ICy (52.7 mg, 0.277 mmol, 4.05 equiv) and stirred for 24 h at room temperature. The solution was filtered through Celite, the solvent was removed in vacuo, and the residue was washed carefully with cold (−40 °C) pentane (3 × 1 mL) and dried in vacuo to give a yellow solid. Yield: 69.3 mg (0.086 mmol, 77%). ^{1}H NMR (CD_2Cl_2, δ): 6.75 (s, 4H, N(C*H*)$_2$N), 5.66 (app t, $^3J_{HH}$ = 11.7, 4H, NC*H*(CH$_3$)$_2$), 2.39−0.59 (m, 62H). ^{13}C{^{1}H} NMR (CD_2Cl_2, δ): 182.7 (Ir−C), 116.1 (N(CH)$_2$N), 59.0 (CH-(CH$_3$)$_2$), 36.0, 35.0, 34.2, 32.2, 30.9, 27.0, 26.7, 26.1. Anal. Calcd for $C_{38}H_{70}N_4IrCl$: C, 56.87; H, 7.79; N, 6.98. Found: C, 56.74; H, 7.87; N, 6.89. Crystals suitable for X-ray diffraction studies were grown by chilling a pentane solution to −40 °C.

$[IrCl(\eta^2\text{-COE})(IDD)_2]$ (8e). Benzene (3 mL) was added to solid $[IrCl(\eta^2\text{-COE})_2]_2$ (99.5 mg, 0.111 mmol) and IDD (191.8 mg, 0.479 mmol, 4.31 equiv) and stirred for 5 days at room temperature. The solution was filtered through Celite, the solvent was removed in vacuo, and the residue was washed carefully with cold (−40 °C) pentane (3 × 1 mL) and dried in vacuo to give a yellow solid. Yield: 171.5 mg (0.150 mmol, 68%). ^{1}H NMR (CD_2Cl_2, δ): 6.77 (s, 4H, N(C*H*)$_2$N), 5.91−5.79 (m, 4H, NC*H*R$_2$), 2.24−1.18 (m, 98H), 1.16−1.10 (m, 2H), 0.85−0.71 (m, 2 H). ^{13}C{^{1}H} NMR (CD_2Cl_2, δ): 181.9 (Ir−C), 116.3 (N(*C*H)$_2$N), 57.5 (NCH), 34.9, 30.5, 30.3, 29.9, 26.7, 25.6, 25.4, 23.2, 23.0, 22.9, 22.8. Anal. Calcd for $C_{62}H_{110}N_4IrCl$: C, 65.37; H, 9.73; N, 4.92. Found: C, 65.38; H, 9.61; N, 5.06. Crystals suitable for X-ray diffraction studies were grown by chilling a pentane solution to −40 °C.

$[IrCl(CO)(I^iPr^{Me})_2]$ (9). **8b** (248.7 mg, 0.356 mmol) was dissolved in pentane (50 mL) in a flask fitted with a J. Young tap. The flask was closed, removed from the glovebox, and attached to the Schlenk line. The solution was frozen, the headspace was removed in vacuo, and the solution was thawed under carbon monoxide. This process was repeated an additional two times. The flask was closed and removed from the Schlenk line, and the solution was stirred at room temperature. Within a few hours, the bright yellow solution became very pale and precipitated a pale yellow solid. After 3 days, the solvent volume was carefully reduced to ca. 10 mL in vacuo, and the flask was returned to the glovebox and chilled to −40 °C. The pentane was carefully decanted, and the solid was washed with cold (−40 °C) pentane (2 × 1 mL) and dried in vacuo to yield a pale yellow solid. Yield: 165.8 mg (0.269 mmol, 76%). ^{1}H NMR (C_6D_6, δ): 6.68 (app br s, 4H, C*H*(CH)$_3$), 1.77 (s, 12H, N(CMe)$_2$N), 1.59 (d, $^3J_{HH}$ = 7.2, 12H, CH(C*H*$_3$)$_2$), 1.47 (d, $^3J_{HH}$ = 7.2, 12H, CH(C*H*$_3$)$_2$). ^{13}C{^{1}H}

dx.doi.org/10.1021/ic4018773 | *Inorg. Chem.* 2013, 52, 12674−12681

NMR (C_6D_6, δ): 179.0, 173.5, 123.9 ($N(C(CH_3))_2N$), 53.5 ($NCH(CH_3)_2$), 21.9 ($NCH(CH_3)_2$), 21.8 ($NCH(CH_3)_2$), 10.1 ($N(C(CH_3))_2N$). IR (ν_{CO}, CH_2Cl_2): 1916.6 cm^{-1}. IR (ν_{CO}, hexane): 1929.5 cm^{-1}. Anal. Calcd for $C_{23}H_{40}N_4ClIrO$: C, 44.83; H, 6.54; N, 9.09. Found: C, 44.71; H, 6.70; N, 9.16.

[IrCl(CO)(O_2)(I^iPr^{Me})$_2$] (12). **9** (6.3 mg, 0.010 mmol) was dissolved in CD_2Cl_2 (0.6 mL) in an NMR tube fitted with a J. Young tap. The flask was closed, removed from the glovebox, and attached to the Schlenk line. The solution was frozen, the headspace was removed in vacuo, and the solution was thawed. Oxygen was then introduced into the NMR tube, and the tube was repeatedly inverted using an NMR tube spinner. The sample was analyzed periodically by ^1H NMR spectroscopy. Key signals for this species are recorded below. ^1H NMR (CD_2Cl_2, δ): 5.69 (app br s, 4H, $CH(CH)_3$), 2.25 (s, 12H, $N(CMe)_2N$), 1.60 (d, $^3J_{HH}$ = 7.2, 12H, $CH(CH_3)_2$), 1.55 (d, $^3J_{HH}$ = 6.8, 12H, $CH(CH_3)_2$).

[Ir(CO)(I^iPr^{Me})$_2$(OH)] (13). **9** (93 mg, 0.15 mmol) was dissolved in THF (4 mL), and the solution was stirred over CsOH (45 mg, 0.30 mmol) at room temperature in the glovebox for 24 h. The reaction mixture was filtered through Celite, the solvents were removed, and the product was washed with cold (−40 °C) pentane (2 × 1 mL) and dried in vacuo to give a pale yellow solid. Yield: 78 mg (0.13 mmol, 84%). ^1H NMR (C_6D_6, δ): 6.83 (app br s, 4H, $CH(CH_3)_2$), 1.79 (s, 12H, $N(C(CH_3))_2N$), 1.53 (d, $^2J_{HH}$ = 6.7, 24H, $CH(CH)_3$).$^{13}C\{^1H\}$ NMR (C_6D_6, δ): 182.1, 179.3, 123.5 ($N(C(CH_3))_2N$), 53.3 ($CH(CH_3)_2$), 21.9 ($CH(CH_3)_2$), 10.2 ($N(C(CH_3)_2N$). IR (ν_{CO}, hexane): 1905.0 cm^{-1}. Anal. Calcd for $C_{23}H_{41}N_4IrO_2$: C, 46.21; H, 6.91; N, 9.37. Found: C, 46.38; H, 6.87; N, 9.32.

[Ir(CO)(I^iPr^{Me})$_2$(O_2CPh)] (14). **13** (19.8 mg, 0.032 mmol) and $PhCO_2H$ (4.3 mg, 0.035 mmol, 1.1 equiv) were dissolved in toluene (0.5 mL), and the solution was stirred at room temperature in the glovebox for 3 days. The solvent was removed, and the product was washed with cold (−40 °C) pentane (2 × 0.5 mL) and dried in vacuo. Yield: 20.3 mg (0.029 mmol, 90%). ^1H NMR (C_6D_6, δ): 8.52 (br s, 1H, ArH), 8.36 (d, $^3J_{HH}$ = 6.2, 2H, ArH), 7.15−7.00 (m, 2H, ArH), 6.77 (app br s, 4H, $CH(CH_3)_2$), 1.70 (s, 12H, $N(C(CH_3))_2N$), 1.62 (d, $^2J_{HH}$ = 6.9, 12H, $CH(CH_3)_2$), 1.54 (d, $^2J_{HH}$ = 6.9, 12H, $CH(CH_3)_2$).$^{13}C\{^1H\}$ NMR (C_6D_6, δ): 178.9, 176.9, 169.9 ($PhCO_2Ir$), 138.7 (Ar C), 130.2 (Ar CH), 129.7 (Ar CH), 127.6 (Ar CH) 123.8 ($N(C(CH_3))_2N$), 53.6 ($CH(CH_3)_2$), 22.1 ($CH(CH_3)_2$), 10.1 ($N(C(CH_3)_2N$). IR (ν_{CO}, hexane): 1931.4 cm^{-1}. Anal. Calcd for $C_{30}H_{45}N_4IrO_3$: C, 51.33; H, 6.46; N, 7.98. Found: C, 51.46; H, 6.34; N, 7.91.

[Ir(CO)(I^iPr^{Me})$_2$(OMe)] (15). **13** (20 mg, 0.034 mmol) was stirred in methanol (0.5 mL) at room temperature in the glovebox for 24 h. The reaction mixture was concentrated in vacuo and azeotroped with pentane until an orange solid resulted. The solid was washed with cold (−40 °C) pentane (3 × 1 mL) and dried in vacuo. Yield: 20.0 mg (0.033 mmol, 96%). ^1H NMR (C_6D_6, δ): 6.75 (br s, 4H, $CH(CH_3)_2$), 4.01 (s, 6H, OMe), 1.80 (s, 12H, $N(C(CH_3))_2N$), 1.67−1.44 (m, 24H, $CH(CH_3)_2$). $^{13}C\{^1H\}$ NMR (C_6D_6, δ): 182.0, 178.3, 123.4 ($N(C(CH_3))_2N$), 61.6 (OMe), 53.4 ($CH(CH_3)_2$), 21.9 ($CH(CH_3)_2$), 10.2 ($N(C(CH_3))_2N$). IR (ν_{CO}, hexane): 1906.0 cm^{-1}. Anal. Calcd for $C_{24}H_{43}N_4IrO_2$: C, 47.11; H, 7.08; N, 9.16. Found: C, 46.98; H, 6.90; N, 9.08.

[Ir(CO)(I^iPr^{Me})$_2$(CCPh)] (16). **13** (20 mg, 0.034 mmol) was stirred in phenylacetylene (0.5 mL) at room temperature in the glovebox for 24 h. The reaction mixture was concentrated to an orange oil in vacuo. Cold (−40 °C) pentane (1 mL) was added, and an orange precipitate formed. The liquid was decanted, and the resultant solid was washed with cold (−40 °C) pentane (3 × 1 mL) and dried in vacuo. Yield: 10.3 mg (0.015 mmol, 45%). ^1H NMR (C_6D_6, δ): 7.42−7.36 (m, 2H,ArH), 6.97 (t, $^3J_{HH}$ = 7.7, 2H, ArH), 6.82 (tt, $^3J_{HH}$ = 7.4, 1.28, 1H, ArH), 6.69 (br s, 4H, $CH(CH_3)_2$), 1.79 (s, 12H, $N(C(CH_3))_2N$), 1.66−1.58 (m, 12H, $CH(CH_3)_2$), 1.54−1.44 (m, 12H, $CH(CH_3)_2$).$^{13}C\{^1H\}$ NMR (C_6D_6, δ): 187.9, 176.5, 131.4 (*o*-ArCH), 130.26 (Ir−CC−Ph), 130.1 (ArC), 128.0 (*m*-ArCH), 124.1 (*p*-ArCH), 123.7 ($N(C(CH_3))_2N$), 111.3 (Ir−CC−Ph), 53.5 ($CH(CH_3)_2$), 21.8 ($CHCH_3$), 21.6 ($CHCH_3$), 10.2 ($N(C(CH_3))_2N$). IR (ν_{CO}, hexane): 1927.1 cm^{-1}. Anal. Calcd for $C_{31}H_{45}N_4IrO$: C, 54.60; H, 6.65; N, 8.22. Found: C, 52.02; H, 5.83; N, 8.90.

[Ir(CO)(I^iPr^{Me})$_2$($OSiPh_3$)] (17). **13** (20 mg, 0.034 mmol) and triphenylsilane (8.8 mg, 0.034 mmol) were stirred in toluene (0.5 mL) at room temperature in the glovebox for 16 h. The reaction mixture was concentrated in vacuo to a white solid, which was washed with cold (−40 °C) pentane (3 × 1 mL) and dried in vacuo. Yield: 19.3 mg (0.023 mmol, 66%). ^1H NMR (C_6D_6, δ): 7.9 (d, $^3J_{HH}$ = 7.8, 2H, ArH), 7.73−7.63 (m, 6H, ArH), 7.30 (t, $^2J_{HH}$ = 7.4, 1H, ArH), 7.08 (t, $^2J_{HH}$ = 7.4, 1H, ArH), 6.83 (sept, $^3J_{HH}$ = 7.0, 4H, $CH(CH_3)_2$), 1.78 (s, 12H, $N(C(CH_3))_2N$), 1.45 (d, $^2J_{HH}$ = 7.0, 12H, $CH(CH_3)_2$), 1.21 (d, $^2J_{HH}$ = 7.1, 12H, $CH(CH_3)_2$).$^{13}C\{^1H\}$ NMR (C_6D_6, δ): 185.9, 181.0, 143.8 (ArC), 135.9 (ArCH), 127.1 (ArCH), 123.7 ($N(C(CH_3))_2N$), 53.5 ($CH(CH_3)_2$), 22.3 ($CH(CH_3)_2$), 21.5 ($CH(CH_3)_2$), 10.3 ($N(C(CH_3))_2N$). IR (ν_{CO}, hexane): 1918.0 cm^{-1}. Anal. Calcd for $C_{41}H_{55}N_4IrO_2Si$: C, 57.51; H, 6.47; N, 6.54. Found: C, 57.39; H, 6.35; N, 6.34.

X-ray Crystal Structure Determinations. Table 2 gives details of the data collection and refinement. Full details can be found in the Supporting Information, which includes CIF and INS data. Data were collected at −180 ± 1 °C using a Rigaku MM007 high-brilliance RA generator with a Saturn 70 CCD area detector using ω scans, using Mo Kα radiation (λ = 0.71075 Å). Intensities were corrected for Lorentz−polarization and for absorption. For **8a**, the structure was solved by direct methods and expanded using Fourier techniques. For **8b−e**, the structure was solved by heavy-atom Patterson methods and expanded using Fourier techniques. In all cases, the non-hydrogen atoms were refined anisotropically, and hydrogen atoms were refined using the riding model.

■ ASSOCIATED CONTENT

Ⓢ Supporting Information

Text, figures, tables, and CIF and INS files giving general experimental information and NMR and IR spectra, steric maps, and crystallographic data for **8a−e**. This material is available free of charge via the Internet at http://pubs.acs.org. Crystallographic data for CCDC-948893 (**8a**), CCDC-948894 (**8b**), CCDC-948895 (**8c**), CCDC-948896 (**8d**), CCDC-948897 (**8e**) can be obtained free of charge from The Cambridge Crystallographic Data Centre via www.ccdc.cam.ac.uk/data_request/cif.

■ AUTHOR INFORMATION

Corresponding Author

*E-mail for S.P.N.: snolan@st-andrews.ac.uk.

Notes

The authors declare no competing financial interest.

■ ACKNOWLEDGMENTS

We thank the EPSRC, the ERC (Advanced Investigator Award "FUNCAT" to S.P.N.), and Sasol (stipend to B.J.T.) for financial support. S.P.N. is a Royal Society Wolfson Merit Award holder. We thank Dr. Tomas Lebl and Mrs. Melanja Smith for assistance with NMR spectroscopy and Dr. Alba Collado, Scott Patrick, Dr. Anthony Chartoire, and Adrián Gómez-Suaréz for helpful discussions. This work has made use of the resources provided by the EaStCHEM Research Computing Facility.

■ REFERENCES

(1) Díez-González, S.; Marion, N.; Nolan, S. P. *Chem. Rev.* **2009**, *109*, 3612.

(2) Clavier, H.; Nolan, S. P. *Chem. Commun.* **2010**, *46*, 841.

(3) Nelson, D. J.; Nolan, S. P. *Chem. Soc. Rev.* **2013**, *42*, 6723.

(4) Benhamou, L.; Chardon, E.; Lavigne, G.; Bellemin-Laponnaz, S.; César, V. *Chem. Rev.* **2011**, *111*, 2705.

(5) Brown, J. A.; Irvine, S.; Kennedy, A. R.; Kerr, W. J.; Andersson, S.; Nilsson, G. N. *Chem. Commun.* **2008**, 1115.
(6) Bennie, L. S.; Fraser, C. J.; Irvine, S.; Kerr, W. J.; Andersson, S.; Nilsson, G. N. *Chem. Commun.* **2011**, *47*, 11653.
(7) Frey, G. D.; Rentzsch, C. F.; von Preysing, D.; Scherg, T.; Mühlhofer, M.; Herdtweck, E.; Herrmann, W. A. *J. Organomet. Chem.* **2006**, *691*, 5725.
(8) Rentzsch, C. F.; Tosh, E.; Herrmann, W. A.; Kuhn, F. E. *Green Chem.* **2009**, *11*, 1610.
(9) Lee, H. M.; Jiang, T.; Stevens, E. D.; Nolan, S. P. *Organometallics* **2001**, *20*, 1255.
(10) Hillier, A. C.; Lee, H. M.; Stevens, E. D.; Nolan, S. P. *Organometallics* **2001**, *20*, 4246.
(11) Truscott, B. J.; Nelson, D. J.; Lujan, C.; Slawin, A. M. Z.; Nolan, S. P. *Chem. Eur. J.* **2013**, *19*, 7904.
(12) Scott, N. M.; Dorta, R.; Stevens, E. D.; Correa, A.; Cavallo, L.; Nolan, S. P. *J. Am. Chem. Soc.* **2005**, *127*, 3516.
(13) Scott, N. M.; Pons, V.; Stevens, E. D.; Heinekey, D. M.; Nolan, S. P. *Angew. Chem., Int. Ed.* **2005**, *44*, 2512.
(14) Fortman, G. C.; Jacobsen, H.; Cavallo, L.; Nolan, S. P. *Chem. Commun.* **2011**, *47*, 9723.
(15) Nelson, D. J.; Egbert, J. D.; Nolan, S. P. *Dalton Trans.* **2013**, *42*, 4105.
(16) Fortman, G. C.; Slawin, A. M. Z.; Nolan, S. P. *Organometallics* **2011**, *30*, 5487.
(17) Nelson, D. J.; Truscott, B. J.; Egbert, J. D.; Nolan, S. P. *Organometallics* **2013**, *32*, 3769.
(18) Tang, C. Y.; Smith, W.; Thompson, A. L.; Vidovic, D.; Aldridge, S. *Angew. Chem., Int. Ed.* **2011**, *50*, 1359.
(19) Tang, C. Y.; Smith, W.; Vidovic, D.; Thompson, A. L.; Chaplin, A. B.; Aldridge, S. *Organometallics* **2009**, *28*, 3059.
(20) de Frémont, P.; Scott, N. M.; Stevens, E. D.; Ramnial, T.; Lightbody, O. C.; Macdonald, C. L. B.; Clyburne, J. A. C.; Abernethy, C. D.; Nolan, S. P. *Organometallics* **2005**, *24*, 6301.
(21) Dorta, R.; Stevens, E. D.; Hoff, C. D.; Nolan, S. P. *J. Am. Chem. Soc.* **2003**, *125*, 10490.
(22) Fortman, G. C.; Slawin, A. M. Z.; Nolan, S. P. *Dalton Trans.* **2010**, *39*, 3923.
(23) Poater, A.; Cosenza, B.; Correa, A.; Giudice, S.; Ragone, F.; Scarano, V.; Cavallo, L. *Eur. J. Inorg. Chem.* **2009**, *2009*, 1759.
(24) The values of $\%V_{bur}$ in Table 1 are calculated excluding hydrogen atoms, as per convention,[2] with $\%V_{bur}$ values consistently 3.3(1)% higher if these are included. However, the order of buried volume does not change (i.e., **8e** > **8b** > **8c** > **8d** > **8a**), and the values still cover a very narrow range, implying similar steric properties.
(25) Vaska, L. *Acc. Chem. Res.* **1968**, *1*, 335.
(26) Chang, Y.-H.; Fu, C.-F.; Liu, Y.-H.; Peng, S.-M.; Chen, J.-T.; Liu, S.-T. *Dalton Trans.* **2009**, 861.
(27) Fu, C.-F.; Chang, Y.-H.; Liu, Y.-H.; Peng, S.-M.; Elsevier, C. J.; Chen, J.-T.; Liu, S.-T. *Dalton Trans.* **2009**, 6991.
(28) Burk, M. J.; Crabtree, R. H. *Inorg. Chem.* **1986**, *25*, 931.
(29) Jacobsen, H.; Correa, A.; Costabile, C.; Cavallo, L. *J. Organomet. Chem.* **2006**, *691*, 4350.
(30) Vaska, L.; Chen, L. S. *J. Chem. Soc. D* **1971**, 1080.
(31) Frisch, M. J.; Trucks, G. W.; Schlegel, H. B.; Scuseria, G. E.; Robb, M. A.; Cheeseman, J. R.; Scalmani, G.; Barone, V.; Mennucci, B.; Petersson, G. A.; Nakatsuji, H.; Caricato, M.; Li, X.; Hratchian, H. P.; Izmaylov, A. F.; Bloino, J.; Zheng, G.; Sonnenberg, J. L.; Hada, M.; Ehara, M.; Toyota, K.; Fukuda, R.; Hasegawa, J.; Ishida, M.; Nakajima, T.; Honda, Y.; Kitao, O.; Nakai, H.; Vreven, T.; Montgomery, J. A., Jr.; Peralta, J. E.; Ogliaro, F.; Bearpark, M.; Heyd, J. J.; Brothers, E.; Kudin, K. N.; Staroverov, V. N.; Kobayashi, R.; Normand, J.; Raghavachari, K.; Rendell, A.; Burant, J. C.; Iyengar, S. S.; Tomasi, J.; Cossi, M.; Rega, N.; Millam, J. M.; Klene, M.; Knox, J. E.; Cross, J. B.; Bakken, V.; Adamo, C.; Jaramillo, J.; Gomperts, R.; Stratmann, R. E.; Yazyev, O.; Austin, A. J.; Cammi, R.; Pomelli, C.; Ochterski, J. W.; Martin, R. L.; Morokuma, K.; Zakrzewski, V. G.; Voth, G. A.; Salvador, P.; Dannenberg, J. J.; DapprichS.; Daniels, A. D.; Farkas, O.; Foresman, J. B.; Ortiz, J. V.; Cioslowsk, J.; Fox, D. J.*Gaussian 09*, Revision A.02; Gaussian, Inc.: Wallingford, CT, 2009.
(32) Blake, A. J.; Ebsworth, E. A. V.; Murdoch, H. M.; Yellowlees, L. J. *Acta Crystallogr., Sect. C: Cryst. Struct. Commun.* **1991**, *47*, 657.
(33) Kuwabara, E.; Bau, R. *Acta Crystallogr., Sect. C: Cryst. Struct. Commun.* **1994**, *50*, 1409.
(34) Fulmer, G. R.; Miller, A. J. M.; Sherden, N. H.; Gottlieb, H. E.; Nudelman, A.; Stoltz, B. M.; Bercaw, J. E.; Goldberg, K. I. *Organometallics* **2010**, *29*, 2176.
(35) Herde, J. L.; Lambert, J. C.; Senoff, C. V.; Cushing, M. A. *Inorg. Synth.* **1974**, *15*, 18.